Plexibot: A Homogeneous Modular Robot Framework for Adaptive Locomotion in Unstructured Environments

Kaavya Goel
The Quarry Lane School
Dublin, California, USA
goelkaavya13@gmail.com

Abstract

Modular robots represent a transformative approach to robotic design and unmanned aerial vehicles (UAVs), leveraging the reconfiguration abilities of numerous interconnected modules to achieve versatile and adaptive functionality. This paper presents a solution to the challenges of robustness and adaptability in dynamic, unstructured environments. While prior research in modular robotics has explored either ground-based or aerial systems, there remains a notable gap in the integration of both modalities into a single adaptive platform. Plexibot, a novel modular robot with aerial and terrestrial capabilities, along with a unique docking system and homogeneous design, enables robust adaptability and reconfiguration. Plexibot is designed to support decentralized coordination between modules, inspired by prior consensus-based modular robotic systems. Combined with its possession of both chain-style and mobile reconfiguration, these modules have an almost limitless range of applications.

Keywords

Modular Robots, Consensus-Based Control, Hybrid Locomotion, Docking Mechanism, Unstructured Environments

ACM Reference Format:
Kaavya Goel. 2026. Plexibot: A Homogeneous Modular Robot Framework for Adaptive Locomotion in Unstructured Environments . In *Proceedings of International Journal of Secondary Computing and Applications Research (IJSCAR VOL. 3, ISSUE 2)*. ACM, New York, NY, USA, 7 pages. https://doi.org/10.67149/yhjs2024.5/n7x5q8jm

Keywords

Modular Robots, Homogeneous, Hybrid Locomotion, Docking Mechanism, Unstructured Environments

Figure 1: A snake-like configuration between five modules

1 Introduction

Nature has long inspired humanity's greatest inventions and scientific breakthroughs by providing insight into how to solve complex problems [1][2]. For example, bees link their legs to form living chains in a process called festooning, which is employed when building and repairing honeycomb. Similarly, hundreds of thousands of ants create living bridges and rafts by clinging to one another in order to traverse gaps or floods.

Traditional robotic systems often struggle in unstructured environments due to their fixed morphology and reliance on centralized control. The way bees festoon and ants build living bridges illustrates a principle that modular robots emulate: individual units working together to create large-scale structures whose capabilities grow as they assemble.

Modular robots are robotic systems composed of individual units, or modules, that can connect, disconnect, or reconfigure to perform an unlimited amount of tasks. They share uniform docking interfaces that enable scalability by adding an n number of modules in order to reach new functionalities. By leveraging coordinated self-assembly and automated reconfiguration, these systems can adapt to changing environments or unknown tasks in various unrehearsed settings.

These robotic systems have the potential to pioneer solutions to real-world scenarios such as search and rescue, disaster relief, planetary exploration, and flexible manufacturing. However, current modular robots often face challenges in versatility, applicability, and robustness, limiting their effectiveness in real-world applications.

The mechatronic conceptualization of the mechanical system uses CAD modeling and design analysis to optimize motion and structural performance. By drawing inspiration from biological systems, this approach aims to enhance the autonomy and adaptability of modular robots, expanding their potential uses in areas such as disaster response, exploration, and manufacturing.

IJSCAR VOL. 3, ISSUE 2,

https://doi.org/10.67149/yhjs2024.5/n7x5q8jm

2 Related Work

Yim et al in [3] show how simulation can meaningfully shape real-world behavior by developing a design library with a set of tested motion routines that let their modular robot handle fast, reactive tasks. In a follow-up project with the PolyBot system portrayed in [4], they reveal how a singular modular platform can switch between diverse locomotion and adaptive reconfiguration for complex urban search and rescue scenarios. A framework for legged robots to navigate unstructured terrain has also been presented . A probabilistic roadmap plans the robot's center-of-gravity trajectory and a heuristic footstep planner ensures stable locomotion over uneven terrain. Two search methods to optimize module configurations in flying modular robots have been presented, enabling efficient control of large-scale structures with reduced computational cost [5]. Similarly, in [6], the authors show through extensive testing that their decentralized control method allows a modular gripper to agree on how much pressure to apply, even when starting from different configurations, and exhibiting scalability with increasing units during grasping tasks. It is demonstrated that the strength of decentralized behavior is groups. Their s-bot, scattered randomly at first, can self-assemble and then move a heavy object together toward a target beacon, an early example of manipulation in modular robots. Modularity is examined in extreme settings such as nuclear-decommissioning sites, showing that systems such as Connect-R adapt to unpredictable environments while still facing limits imposed by radiation and intricate control demands [7].

3 System

While prior research in modular robotics has explored either ground-based or aerial systems such as in [8] or [9], there remains a notable gap in the integration of both modalities into a single adaptive platform. The research developed for Plexibot directly addresses this by focusing on homogeneous hybrid modular robots capable of both ground and aerial movement, designed to reconfigure dynamically in response to diverse, unstructured terrains.

3.1 Design Parameters

The three main design expectations for Plexibot were to maintain a reasonable weight, an ability to function in both the air and ground, and to keep a low cost and high manufacturability in terms of materials and parts. To meet these expectations, Plexibot is designed as a hybrid quadrotor-based platform to maneuver both air and ground environments. At the core of the system are four propellers (a quadrotor), mounted symmetrically on a square frame, as shown in Fig. 2. Quadrotors have already been proven to be a lightweight solution to aerial locomotion [9][10][11]. In this case, the propellers serve as the actuators as they generate thrust for both aerial and terrestrial locomotion. Unlike conventional modular robots, this design incorporates a pair of centrally mounted wheels, enabling efficient ground traversal and reducing friction and energy consumption when aerial capability is not required. In order for the propellers to lift off the ground, they have to spin faster, consuming more energy, but the modular aspect compensates for the payload it is lifting by distributing the weight evenly between modules. We can determined that an increase in modules significantly improves battery and increases energy efficiency. The wheels themselves are passive, with no actuators attached, as steering and linear movement are handled entirely by the quadrotor.

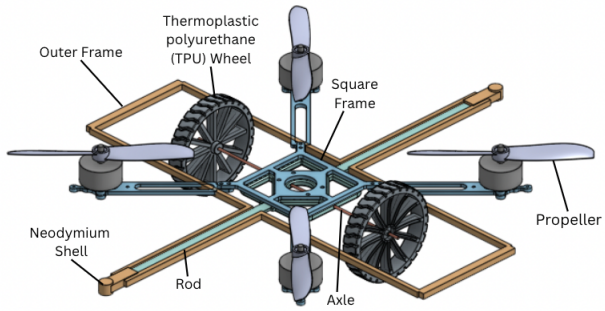

Figure 2: Digital CAD rendering of Plexibot and its design.

The weight of the system was a critical factor in the design process, as payload capacity and energy efficiency are directly tied to overall mass. By minimizing unnecessary bulk and optimizing component placement, the design achieves an optimal magnet-to-weight ratio R, which can be computed as follows

$$R = \frac{F_{\text{mag}}}{m_{\text{robot}} \cdot 9.81}$$

where F_{mag} is the magnetic force in weight unit and m_{robot} is the robot mass. Each cylindrical neodymium magnet has a pull force of 8 lbs (35.6 N) and the mass of each module is 134.96 g. We get a magnet-to-weight ratio of 1:26.9, meaning that each module's magnet can hold around 26.9 times its own weight. The large acceptance region margin relative to module weight results in a wide docking tolerance, allowing the system to self-correct under moderate positional and angular misalignment during attachment. This poses an angular tolerance of up to 34°, and a lateral tolerance of 6 mm.

Another factor in weight reduction was selecting a frame material of PLA [12][13], chosen for its manufacturability and low density. Aero PLA provides an excellent strength-to-weight ratio for a proof-of-concept design, while its ease of manufacturing supports rapid iteration and feasibility. The use of PLA in general also makes the design cost-effective and easily reproducible, an important consideration for the application of Plexibot.

3.2 Overall Structure

The overall design of Plexibot (refer to Fig. 2) consists of a square 70x75 mm PLA frame with four propellers mounted on it. The four propellers mounted on the main frame are jointly a quadrotor. The quadrotor serves two main purposes: aerial and terrestrial locomotion. While on the ground, the wheels serve only as a means of rolling contact, whereas the quadrotor functions as the primary actuator, generating the force required to move the system back and forth. With low-inertia wheels, the torque is negligible, so the rotational kinetic energy created in the air is too small to generate any meaningful gyroscopic effect. Similarly, the actuators and propellers are positioned to maintain equal weight distribution across

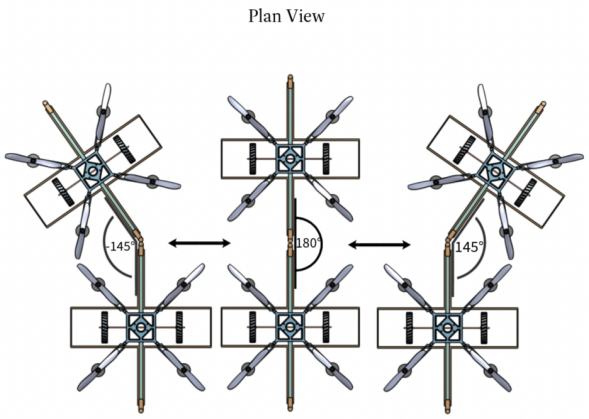

Figure 3: Top view of three distinct configurations. The modules are able to pivot or rotate around the cylindrical magnets' shell. The intermodular angles, measured from left to right, are -145°, 180°, and 145°, respectively. The arrow between modules indicates that Plexibot can transition between configurations, subject to a design constraint limiting rotation to 145° before two quadrotors make contact.

the frame, preventing torque imbalances and ensuring consistent performance in both aerial and terrestrial modes.

An axle with a 2 mm diameter runs through the frame horizontally with a wheel attached at each end. A major focus of the design lies in the wheel system, which is engineered to maximize terrestrial performance while minimizing additional weight. The large wheels have a diameter of 80 mm and are modeled after off-the-road (OTR) rubber tracks featuring a straight lug tread pattern. This was chosen for their enhanced traction and durability on uneven, varied surfaces. This is essential for Plexibot to operate during unstructured environments. Although capable of handling rough terrain, the modular robot is carefully designed to remain hollow and lightweight, avoiding unnecessary mass that would otherwise reduce flight time. Their placement at the center of the robot ensures balanced load distribution, reducing stress on the frame and improving rolling efficiency. In addition, the design choice of two wheels better supports the snake-like configuration shown in Fig. 1. It also prevents excessive tilting or instability during transitions between flight and ground modes.

The defining mechanism of the modular robot is its novel self-aligning docking mechanism, which allows the interconnected network of modules to form. Along the axis orthogonal to the wheels are magnets encapsulated in a hollow cylindrical shell positioned vertically. Each cylindrical magnet has a diameter of 9.525 mm (3/8 in).

3.3 Cylindrical Magnets

The three design parameters implemented in the magnets were high attraction force, large surface area, and ability to rotate. The high attraction force and large surface area ensured the two modules stayed securely attached during flight. Neodymium magnets (NdFeN) were selected due to their status as the strongest commercially available magnetic material [14], providing exceptionally high attraction forces and reducing the risk of breakage upon impact with other modules. Their ease of sourcing also supported their selection for this application. The original design was a sphere because it would allow the modules to rotate in all directions, but the low surface area made it impractical for aerial locomotion. The cylindrical magnet allows for one axis of freedom and a higher surface area, enabling better stability while in the air. The importance of the magnetic connection of modular robots and the exploration of their different structures are shown in [15]. This axis of freedom allows for snake-like movements and high maneuverability in both aerial and terrestrial locomotion. Three different interactions or configurations between two modules are shown in Fig. 3. If a cylindrical magnet stands vertically, cutting it along its height yields two halves with opposite magnetic poles. The concept is that the cylindrical magnets rotate freely within the shell, and when two modules approach each other, they orient themselves so that their opposite poles attract. In earlier designs, the magnets were fixed in place, meaning only one of the four sides could successfully dock, forcing each module to turn 180° around to connect. The proposed design allows a module to rotate a maximum of 90° in any direction, making movements simpler and more efficient. The movement of the cylinders are shown in Fig. 4.

3.4 Distributed Coordination Framework

Plexibot modules coordinate using a lightweight distributed consensus mechanism inspired by prior modular robotics work [6]. Each module periodically broadcasts its local state vector *si*=(*pi, vi, mi*) containing position, velocity, and module status. Neighboring modules update their control commands using a consensus update rule

$$u_i(t+1) = u_i(t) + \alpha \sum_{j \in N_i} \big(u_j(t) - u_i(t)\big)$$

where Ni represents neighboring modules within communication range and alpha is a gain parameter controlling convergence speed. This allows modules to converge on shared behaviors such as coordinated docking, cooperative payload lifting, or collective navigation without relying on a centralized controller.

4 Docking and Undocking

4.1 Docking Action

Docking is a crucial part of Plexibot, because it is the method in which modules can join an interconnected network that can help complete more extensive tasks. Docking between modular units involves aligning and coupling two robotic modules. This process is actuated by a quadrotor, which applies an external force F. Figs. 5-7 models the system in two dimensions.

Before the modules initiate docking, their propellers are presumably powered down (where $\vec{F}_1$ and $\vec{F}_2$ equal 0). In this unactuated state (shown in Fig. 5), the modules naturally come to rest in a tilted orientation, supported by one of its lateral faces. This position serves as the starting point for subsequent steps, such as reaching equilibrium.

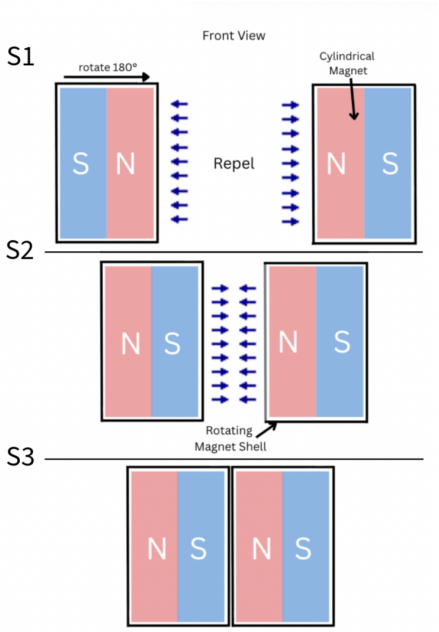

Figure 4: The magnets rotate freely inside the shell until opposite poles face each other and attract. The first stage has both north poles facing each other, and therefore repel. In stage 2, one of the magnets have rotated so that opposite poles are facing each other and there is an attraction force between them. In stage 3, the magnets are attached as a result of the attraction force in stage 2.

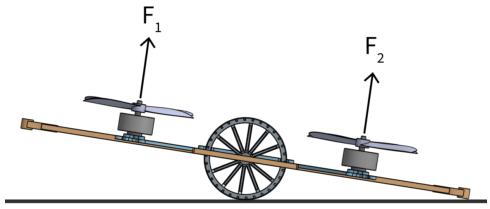

Figure 5: A single module resting in a tilted orientation, supported by one of its lateral faces, as a result of the quadrotor being is powered off.

The magnitudes of the contact forces are computed using the Euclidean norm:

$$\|F_1\| = \sqrt{f_{1x}^2 + f_{1y}^2}, \qquad \|F_2\| = \sqrt{f_{2x}^2 + f_{2y}^2}$$

The vector $\vec{F}_1$ represents the total force acting on the module in Stage 1 of docking and its direction. Its components along the x- and y-directions are denoted by F_{1x} and F_{1y}, respectively.

$$\vec{F}_1 = \begin{bmatrix} F_{1x} \\ F_{1y} \end{bmatrix}$$

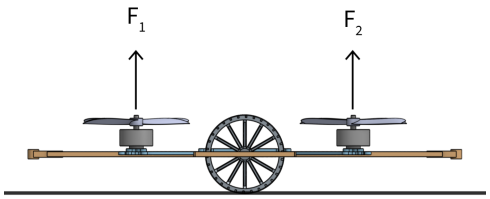

Figure 6: The module at equilibrium.

$$\vec{F}_2 = \begin{bmatrix} F_{2x} \\ F_{2y} \end{bmatrix}$$

Because the modules are homogeneous, we can assume that all modules have the same mass or that $m = m_a = m_b$.

We define forces for modules A and B as follows:

F = External force applied by quadrotor (N)
F_1, F_2 = Contact forces on modules 1 and 2 (N)
f_{1x}, f_{1y} = Components of F_1 (horizontal and vertical)
f_{2x}, f_{2y} = Components of F_2 (horizontal and vertical)
M = Resulting moment (torque) about system center (Nm)
d = Distance from system center to module contact point (m)
m = Mass of each module in g
g = Gravitational acceleration (9.81 m/s^2)
μ = Coefficient of static friction between module and ground
F_{ROLL} = Force that resists motion, encompassing friction.

The condition $F_{1y} + F_{2y} < m \cdot g$ must be satisfied to keep the modules on the ground. This constraint runs through all stages of docking. To correct for the tilt of the quadrotor, $\vec{F}_{2y}$ must be greater than $\vec{F}_{1y}$. This imbalance creates a moment [16] that rotates the module back towards equilibrium. In this context, a moment is the turning effect produced when a force acts at a distance from the pivot point, such as gravity acting on the robot's offset center of mass while it is tilted. Moment can be represented using the variable M. When $F_{2y} > F_{1y}$, the equation

$$M = F_{2y} \cdot d - F_{1y} \cdot d = d(F_{2y} - F_{1y})$$

generates a nonzero moment ($M \neq 0$). This moment drives the rotation until the forces balance and the system reaches equilibrium as shown in Fig. 6. A difference between the vertical forces on each side produces a net moment that rotates the module toward equilibrium.

Once the quadrotor is parallel to the ground, the speed in which the propellers are spinning equals out, and the equation

$$F_{1y} = F_{2y}$$

will be applied. This roll and pitch actuation motion can also be applied in order to maintain equilibrium while navigating rough terrain. The lift and lateral movement force supplied by the quadrotor

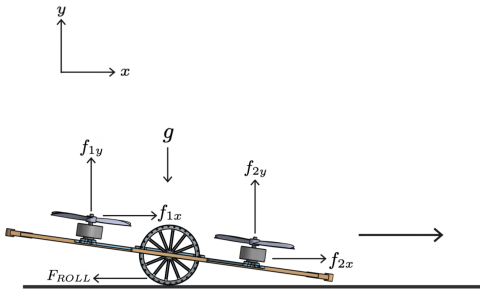

Figure 7: F_{1y} exceeds F_{2y} and generates a nonzero moment that will allow this module to accelerate towards the second module

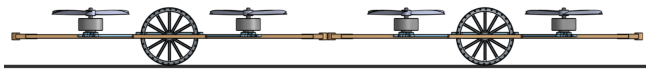

Figure 8: The two modules are now fully aligned and docked together.

also decreases contact with rough terrain, offering a robust solution to unstructured environments.

Moment-Driven Maneuvers. Once equilibrium has been reached, controlled forces can be applied to induce motion. If the vertical force in F_{1y} exceeds that in F_{2y}, the resulting moment causes the module to rotate allowing it to move toward alignment for docking. F_{1y}, F_{2y}, F_{1x}, and F_{2x} must all be greater than 0 during this process.

$$F_{1x} + F_{2x} > F_{ROLL}$$

is also a constraint; otherwise, forces such as friction would resist the module's horizontal motion. The maximum available static friction is defined as:

$$F_{\text{friction}} = \mu(f_{1y} + f_{2y})$$

As the difference between F_{1y} and F_{2y} increases, the tilt becomes more aggressive, resulting in a larger x-component of motion, and a faster acceleration. In order to create sharp turns, the module can fly, applying yaw actuation which will induce rotation around its z-axis. Once the desired angle is achieved, F_{1y} and F_{2y} become equal again, resulting in a moment. The direction and speed in which the module travels can be controlled by the increase or decrease of vertical forces on a specific side. These steps of motion are sustained until the two modules are successfully docked together. The air actuation, along with docking and undocking of aerial modular robots can be seen in [17][18]. The process by which an aerial modular robot consisting of a quadrotor design can grip objects is described in [19]

4.2 Undocking Action

The undocking phase involves the separation of two previously connected modular units by reversing the conditions needed for docking. Undocking requires overcoming the attractive forces between modules, which is assisted by active actuation. The magnets are disconnected in a sort of shearing action, where they are pulled in opposite vertical directions in order to break attraction. It typically occurs when a task has been completed or when the system needs to reconfigure. The modules start out docked, connected by the cylindrical magnets, as shown by Fig. 8. A new set of forces can now be defined:

f_{1x}^A, f_{1y}^A = Components of force F_1 acting on module A (N)
f_{2x}^A, f_{2y}^A = Components of force F_2 acting on module A (N)
f_{1x}^B, f_{1y}^B = Components of force F_1 acting on module B (N)
f_{2x}^B, f_{2y}^B = Components of force F_2 acting on module B (N)
$F_{\text{attraction}}$ = Magnetic attraction force between modules (N)

To initiate undocking, there are a series of conditions that must be followed. The total horizontal forces acting on both modules must exceed the attractive force between them:

$$f_{1x}^A + f_{2x}^A + f_{1x}^B + f_{2x}^B > F_{\text{attraction}}$$

Each module must individually overcome friction to begin sliding apart:

$$f_{1x}^A + f_{2x}^A > F_{\text{ROLL}}, \qquad f_{1x}^B + f_{2x}^B > F_{\text{ROLL}}$$

The magnitude of the resultant forces for each contact is:

$$\|F_1^A\| = \sqrt{(f_{1x}^A)^2 + (f_{1y}^A)^2}, \qquad \|F_2^A\| = \sqrt{(f_{2x}^A)^2 + (f_{2y}^A)^2}$$

$$\|F_1^B\| = \sqrt{(f_{1x}^B)^2 + (f_{1y}^B)^2}, \qquad \|F_2^B\| = \sqrt{(f_{2x}^B)^2 + (f_{2y}^B)^2}$$

Because the modules are now together, the old constraint of $F_{1y}+F_{2y} < m \cdot g$ does not apply anymore. Because we are accounting for the mass of both modules, we get the equation:

$$f_{1x}^A + f_{2x}^A + f_{1x}^B + f_{2x}^B < 2 \cdot m \cdot g$$

f_{2y}^A has to be greater than f_{1y}^B, because that is what creates the shearing effect shown in Fig. 10.

The shear force shown is the internal force acting parallel to the cross-section of an object, which tends to cause parts of the object to slide or deform laterally. The shear-force coefficient C falls within the range $0.4 < C < 0.75$, meaning the shear force is about 0.4-0.75 times the normal pull force (which is 8 lbs for each neodymium magnet). We can introduce two new variables:

$F_{ATT,S}$ = The shear force
$F_{ATT,N}$ = Normal Pull Force

$$F_{ATT,S} = C \cdot F_{ATT,N}$$

Despite the generous angular and lateral tolerances of the cylindrical magnet design, docking success depends on controlled approach conditions. High relative velocity, misalignment beyond the 34° threshold, or environmental disturbances such as uneven terrain or airflow represent potential failure modes that may reduce attachment reliability. Debris or surface irregularities could also

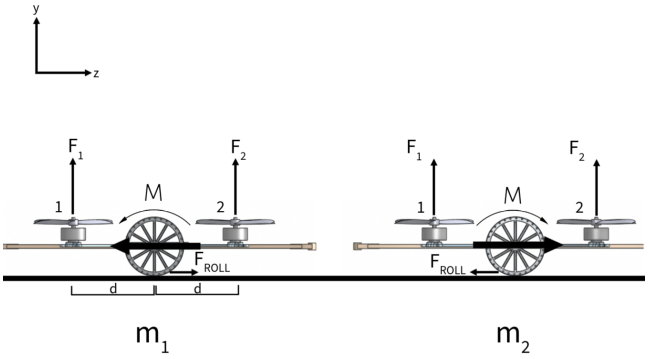

Figure 9: The undocking process, with all forces acting on the two modules indicated. The rods move vertically in opposite directions to create the shearing motion that separates the two cylindrical magnets.

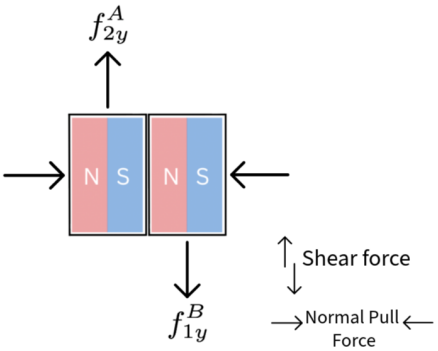

Figure 10: A shearing motion acting on the cylindrical magnets, with one moving upward and the other downward. This motion opposes the normal attractive force shown by the inward-facing horizontal arrows.

interfere with full magnetic contact, highlighting the importance of sensor-informed alignment during docking.

5 Applications

The proposed design has a wide range of applications across fields that demand mobility, adaptability, and coordinated behavior in unpredictable environments. In disaster response, individual modules could fly over collapsed structures to identify viable entry points, then transition to wheel-based motion to move through narrow gaps without consuming excessive power. Once inside unstable rubble, multiple units could dock side-by-side to form a chain capable of threading through narrow gaps. A vertically stacked configuration could operate as a thermal sensor, raising cameras or microphones above debris layers to detect survivors. During post-disaster recovery, docked chains could function as temporary support beams, while free modules deliver essential items such as first-aid kits or communication devices to responders by gripping a payload. In order to lift a payload, modules would dock together and arrange around the object, forming a tight ring-like structure that would then lift into the air.

In construction and architectural settings, flight-enabled modules could lift components such as insulation panels, wiring bundles, bricks, or small structural connectors to elevated workspaces. Docked groups could create temporary handrails or stabilizing rails along unfinished walkways. A chain of modules could also transport tools or materials across the site by rolling in ground mode, reducing the need for workers to repeatedly relocate equipment.

This same ring-like configuration could also perform tasks such as retrieving parts from bins, transporting them to assembly stations, and sorting finished components by placing them in designated zones. When arranged into longer chains, they could shuttle materials across the floor or reposition fixtures that require stable handling.

In environmental monitoring, flight mode enables rapid deployment across remote or uneven terrain. Once dispersed, modules could transition to ground mode to carry out stable sampling tasks, such as lowering pH probes into soil or collecting water samples with small integrated canisters. The lightweight PLA frame allows for large-scale deployment, enabling distributed monitoring networks tailored to specific habitats. As advancements in cooperative flight control, lightweight propulsion, and autonomous docking continue, the system could be further developed for planetary exploration. On the Moon or Mars, modules could fly short hops in low gravity to traverse craters or rocky fields, then dock to create stable platforms for placing instruments, supporting small payloads, or lifting regolith samples.

6 Results

The performance of Plexibot was evaluated through simulation and CAD-based analysis, focusing on docking efficiency, stability, payload capacity, and mobility. The three design parameters for Plexibot were to maintain a reasonable weight, an ability to function in both the air and ground, and to keep a low cost and high manufacturability in terms of materials and parts. Docking simulations demonstrated that the modules successfully aligned and connected in under five seconds on average, with the self-aligning cylindrical magnets reliably ensuring correct orientation without manual adjustment. Stability tests indicated that modules maintained equilibrium when tilted up to 30° without slipping or unintended rotation, confirming the effectiveness of the calculated moments and force distributions. The magnet-to-weight ratio of 26.9:1 allowed modules to collectively lift objects up to 25 times their individual mass when docked in a ring configuration, highlighting the system's capability for cooperative payload handling. The hybrid locomotion system enabled smooth transitions between aerial and ground modes, with ground-mode friction and rolling resistance within expected operational limits, demonstrating both energy efficiency and maneuverability. Overall, these results suggest that Plexibot can effectively adapt to unstructured environments and coordinate multiple modules to complete complex tasks.

7 Conclusion

In conclusion, modular robots represent a transformative approach to robotics, combining flexibility, scalability, and adaptability in ways traditional robots cannot match. Their ability to reconfigure both on the ground and in the air allows them to perform diverse tasks, from cooperative load lifting and structural assembly to navigation in complex environments. The unique characteristics of modular designs, such as homogeneous modules, versatile docking mechanisms, and distributed coordination, enable these systems to adapt seamlessly to new challenges, making them highly applicable across architecture, exploration, and industrial tasks. As research continues to refine their control algorithms, energy efficiency, and hybrid mobility, modular robots are poised to redefine the boundaries of autonomous, collaborative, and multifunctional robotic systems. This paper presents Plexibot as a theoretical framework and mechanical design. A typical quadrotor module operating at this scale consumes approximately 8–12 W during hover. With a 2-cell LiPo battery (approximately 7.4 V, 850 mAh), a single module could sustain flight for roughly 6–8 minutes under nominal payload conditions. Ground-mode locomotion significantly reduces power consumption since thrust requirements are lower than full lift. Future work will further explore the flight control architecture responsible for regulating propeller speeds and maintaining stability, building upon the embedded flight control system that integrates IMUs, an optical flow–based velocity and altitude sensing module, and a multi-directional time-of-flight distance sensing module. Future development will focus on improving how these onboard sensors are fused to maintain balance, adapt to changing payload distributions, and ensure stable operation when multiple modules are connected. Expanded use of optical flow and proximity measurements will enhance docking precision, obstacle awareness, and smooth transitions between aerial and ground movement. Inter-module coordination can be further developed through wireless communication using separate frequency channels to ensure synchronized behavior when needed, complementing the existing mechanical alignment that supports passive state consistency during docking.

References

[1] D. Saldana, B. Gabrich, G. Li, M. Yim, and V. Kumar, "Modquad: The flying strucuture that self-assembles in midair," in *IEEE International Conference on Robotics and Automation 2018*, Brisbane, Australia, 2018.

[2] P. Swissler and M. Rubenstein, "Fireant: A modular robot with full-body continuous docks," in *2018 IEEE International Conference on Robotics and Automation (ICRA)*, 2018, pp. 6812–6817.

[3] M. Yim, Y. Zhang, and D. Duff, "Modular robots," *IEEE Spectrum*, vol. 39, no. 2, pp. 30–34, 2002.

[4] M. Yim, D. Duff, and K. Roufas, "Modular reconfigurable robots, an approach to urban search and rescue," in *Proc. of the HUman Welfare-friendly Robotic Systems Workshop (HWRS), (invited)*, Taejon, Korea, January 2000.

[5] B. Gabrich, D. Saldaña, and M. Yim, "Finding structure configurations for flying modular robots," in *2021 IEEE/RSJ International Conference on Intelligent Robots and Systems (IROS)*. IEEE, 2021, pp. 6970–6976.

[6] C.-H. Yu and R. Nagpal, "Self-adapting modular robotics: A generalized distributed consensus framework," in *2009 IEEE International Conference on Robotics and Automation*. IEEE, 2009, pp. 1881–1888.

[7] M. E. Sayed, J. O. Roberts, K. Donaldson, S. T. Mahon, F. Iqbal, B. Li, S. Franco Aixela, G. Mastorakis, E. T. Jonasson, M. P. Nemitz *et al.*, "Modular robots for enabling operations in unstructured extreme environments," *Advanced Intelligent Systems*, vol. 4, no. 5, p. 2000227, 2022.

[8] C. Liu, Q. Lin, H. Kim, and M. Yim, "SMORES-EP, a modular robot with parallel self-assembly," *Autonomous Robots*, 2022. [Online]. Available: https://doi.org/10.1007/s10514-022-10078-1

[9] B. Gabrich, G. Li, and M. Yim, "Modquad-dof: A novel yaw actuation for modular quadrotors," in *IEEE International Conference on Robotics and Automation 2020, to be presented*, Paris, France, 2020.

[10] G. Li, B. Gabrich, D. Saldana, J. Das, V. Kumar, and M. Yim, "Modquad-vi: A vision-based self-assembling modular quadrotor," in *IEEE International Conference on Robotics and Automation 2019*, Montreal, Canada, 2019.

[11] B. Gabrich, D. Saldana, V. Kumar, and M. Yim, "A flying gripper based on cuboid modular robots," in *IEEE International Conference on Robotics and Automation 2018*, Brisbane, Australia, 2018.

[12] K. Mitsuhashi, Y. Ohyama, H. Hashimoto, and S. Ishijima, "Production and education of the modular robot made by 3d printer," in *2015 10th Asian Control Conference (ASCC)*, 2015, pp. 1–5.

[13] D. Krupke, F. Wasserfall, N. Hendrich, and J. Zhang, "Printable modular robot: an application of rapid prototyping for flexible robot design," *Industrial Robot: the international journal of robotics research and application*, vol. 42, no. 2, pp. 149–155, 03 2015.

[14] P. G. Shewane, M. Gite, A. Singh, and A. Narkhede, "An overview of neodymium magnets over normal magnets for the generation of energy," *International Journal on Recent and Innovation Trends in Computing and Communication*, vol. 2, no. 12, pp. 4056–4059, 2014.

[15] M. Uğur, Y. Yaman, B. Arslan, Çağrı Ergin, and O. Özcan, "Relmbot: A reconfigurable, legged, miniature, modular robot with compliant or rigid, magnetic connection mechanisms," *IEEE Robotics and Automation Letters*, vol. 10, no. 11, pp. 11 737–11 744, 2025.

[16] S. Ding, L. Liu, and W. X. Zheng, "Sliding mode direct yaw-moment control design for in-wheel electric vehicles," *IEEE Transactions on Industrial Electronics*, vol. 64, no. 8, pp. 6752–6762, 2017.

[17] F. Forte, R. Naldi, A. Serrani, and L. Marconi, "Control of modular aerial robots: Combining under- and fully-actuated behaviors," in *2012 IEEE 51st IEEE Conference on Decision and Control (CDC)*, 2012, pp. 1160–1165.

[18] D. Saldaña, P. M. Gupta, and V. Kumar, "Design and control of aerial modules for inflight self-disassembly," *IEEE Robotics and Automation Letters*, vol. 4, no. 4, pp. 3410–3417, 2019.

[19] V. Ghadiok, J. Goldin, and W. Ren, "Autonomous indoor aerial gripping using a quadrotor," in *2011 IEEE/RSJ International Conference on Intelligent Robots and Systems*, 2011, pp. 4645–4651.

Received 19 January 2026; Accepted 20 March 2026